16th World Conference on Earthquake Engineering, 16WCEE 2017

Santiago Chile, January 9th to 13th 2017

Paper N° ID: 2272

Registration Code: S-C1463058170

AN APPLICATION OF FRP SYSTEM FOR THE FLEXURAL SEISMIC RETROFIT OF REINFORCED CONCRETE BEAMS

J. Bazan(1) and V.I. Fernandez-Davila(2).

(1) *Research Engineer, Facultad de Ingeniería Civil. Universidad Nacional de Ingeniería. Lima. Peru, jorgelbs87@hotmail.com*
(2) *Professor, Facultad de Ingeniería Civil. Universidad Nacional de Ingeniería. Lima. Peru, vifdavila@uni.edu.pe*

Abstract

The design and construction of structural retrofit on concrete reinforced elements is an applied engineering field that is growing and developing new techniques.

Among the modern techniques of structural strength, we have the use of externally bonded systems, like the FRP systems. This new technique of retrofit concrete reinforced structures is highly regarded and accepted around the world due to its light weight, high resistance and anticorrosive properties.

The FRP system has a linear elastic behavior of stress-strain to the ultimate failure without any ductility. This characteristic suggests a serious limitation on its applicability to seismic-resistant structures, where it is expected that the seismic energy is dissipated by the inelasticity of materials. Beams externally strengthened with FRP have a more fragile behavior than a respective beam without an external FRP system.

The ductility of a concrete reinforced beam externally strengthened with an FRP system is limited by the amount of steel reinforcement and the FRP system used, this can lead to different failures modes, some could be ductile and others more fragile.

The present study shows the feasibility of the use of FRP systems in strengthened concrete reinforced elements by bending in seismic resistant applications, from the analysis of the ductility feature derived from moment-curvature curve. The main objectives of this study were: to identify characteristics of an FRP system for external retrofit and to identify which features from the beam impact in the seismic-resistant behavior. Another objective was to propose a practical approach to estimate the beam capacity to reach an acceptable ductile failure mode when a beam was externally strengthened with a specific FRP system; experimental tests were carried out on full-scale prototypes of reinforced concrete beams in order to corroborate the results.

The experimental tests were carried out using 6 reinforced concrete beam prototypes, built to full-scale. The beams had a rectangular cross section of 200 x 400 mm^2, with a total span of 2700 mm. The beams were reinforced internally with longitudinal bars of steel reinforcement quality ASTM A615 grade 60; the amounts provided were 0.86%, 1.42% and 2.53%. The specific concrete resistance reached f'_c= 32 MPa. The external FRP for strengthening were formed by laminated layers of 200 mm wide by 1 mm thick and extended along the tensile zone to a length of 2300 mm. The tests took place in the Structures Laboratory of the Centro Peruano Japonés de Investigaciones Sísmicas y de Mitigación de Desastres (CISMID) of the Universidad Nacional de Ingeniería. These tests were by pure bending and allowed calculating the experimental ductility under pseudo-static conditions, and permitted us to corroborate the analytical results.

The study concludes that there are limited ranges of strengthening with an FRP system, which allow the development of an acceptable ductility for a specified concrete reinforced beam (3 to 5), and indicates how to estimate this range. Additionally this study looks to propitiate the investigation of FRP for seismic applications on strengthened concrete reinforced beams by bending.

Keywords: Ductility, FRP, ratio of reinforcement, failure mode, elastic modulus

1. Introduction

The FRP external reinforcement methods for bending on beams develop more fragile systems where ductility is reduced and even lost completely; depending on the conditions of the external reinforcement system.

This paper shows a practical method to identify and / or predict the performance characteristics expected to reinforce an element type of reinforced concrete beam. The failure mode and the resulting ductility are the main points of interest. In this way, the conditions will be known in order to obtain a reasonably ductile bending system, when external strengthening with an FRP system is used on a beam of reinforced concrete. For this purpose, the external reinforcement configurations and the resulting bending ductility are studied from the moment curvature curve.

Finally, the methodology consists of: i) study the states of deformation at yield and ultimate limit, ii) determine the expressions to identify failure modes, and iii) validate the results by experimental tests. The characteristics that are favorable for obtaining acceptable ductility in systems externally reinforced with FRP and appropriate ranges of external reinforcement were determined with the formulation of the expressions for calculating the failure mode and with estimating flexural ductility, respectively.

2. Research Significance

The goal is to obtain the conditions and range of reinforcement that allow for limited ductility in three to five units in externally strengthened reinforced concrete beam systems, for applications in seismic retrofit of buildings.

3. Methodology

Equations arising both on the use and efficiency of FRP, failure modes and ductility associated with this system allow us to identify the variables and the properties of the materials studied that are favorable for a desired ductile behavior in bending reinforced concrete beams with external FRP for strengthening.

3.1. Using FRP system efficiently

The limitations in the design of FRP material occur by the deformation that prevents failure by the delamination or debonding of the FRP band (ε_{fd}) from concrete substrate, not by the ultimate strength. Generally this effective deformation controls the design of the reinforcement, over the ultimate deformation $\varepsilon_{fd} < \varepsilon_{fu}$.

Because this design methodology is limited to the debonding strain of externally bonded FRP reinforcement (ε_{fd}), the entire tension capacity of the material cannot be used, and thus the ultimate strength of the composite system (ε_{fu}) does not represent the parameter comparison between two different reinforcement systems. In reviewing the theoretical equation for calculating the strain of the FRP system during debonding or delamination from concrete substrate [1], it is noted that this mainly depends on the quality of the concrete and the relative rigidity of the FRP system.

$$\varepsilon_{fd} = 0.41\sqrt{\frac{f'_c}{n_f\, E_f\, t_f}} \leq 0.9\varepsilon_{fu} \tag{1}$$

So when evaluating the implementation of different reinforcement systems FRP, these systems must be evaluated based on their equivalent axial rigidity (K_f), also we can check which system is more efficient when comparing the debonding strain of externally bonded FRP reinforcement (ε_{fd}), with the rupture strain of FRP reinforcement (ε_{fu}).

$$K_f = n_f \, E_f \, t_f \tag{2}$$

So the most efficient systems in an application critical adherence are those under the same condition f'_c, and which have a low relative stiffness $E_f.t_f$, and a few layers of reinforcement (n_f). The use of transverse clamps along the longitudinal reinforcement improves performance regarding deformation predicted by Eq. (1). A 30% increase of the debonding strain of externally bonded FRP reinforcement has been observed in various tests [2].

3.2. Identification of failure modes

Based on an analysis of the section of a reinforced concrete beam in its ultimate state for different failure modes, we can identify pre-existing conditions and corresponding external reinforcement. It used a similar approach to that proposed by Banks [3] to define failure modes.

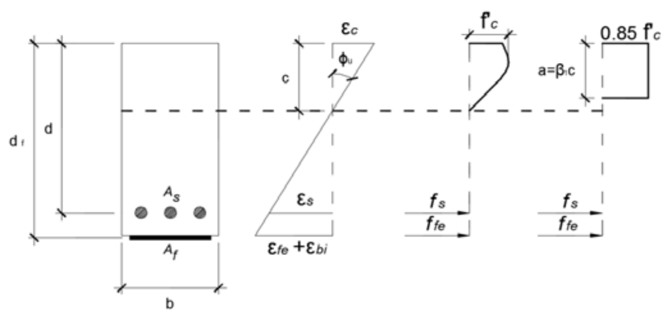

Figure 1: Internal strain and stress distribution for a rectangular beam under bending at ultimate state.

3.2.1. Failure Mode A and B: Steel yield followed by failure in the FRP system.

The balanced condition is analyzed where concrete ($\varepsilon_c = \varepsilon_{cu}$) and the FRP system ($\varepsilon_{fe} = \varepsilon_{fd}$) fail simultaneously. During this balanced condition, the reinforcing steel is generally in yield ($\varepsilon_s \geq \varepsilon_y$) [4].

From the compatibility between strains and stresses the following equations (Eqs. (3) to (5)) can be obtained.

$$\frac{a}{\beta_1 d_f} = \frac{\varepsilon_{cu}}{\varepsilon_{cu} + \varepsilon_{fe} + \varepsilon_{bi}} \tag{3}$$

Making the balance of internal forces between concrete, steel and FRP, we have the following relations:

$$C = T_s + T_f \tag{4}$$

$$0.85\, f'_c \, b \, a = A_s \, f_y + n_f b_f \, t_f \, E_f \, \varepsilon_{fe} \tag{5}$$

ρ_f is defined as the ratio of fiber applied to a section of reinforced concrete and is expressed as the ratio of the total area of FRP used and the effective area of the section, as shown in Eq. (6)

$$\rho_f = \frac{n_f b_f t_f}{b.d} \tag{6}$$

The equation for ρ_f is obtained from Eq. (5) by replacing the amount of external FRP reinforcement with the reinforced concrete system which achieves a balanced mode of failure ($\varepsilon_{fe} \geq \varepsilon_{fd}$).

$$\rho_f = \frac{0.85\, f'_c\, a}{E_f\, \varepsilon_{fd}\, d} - \rho_s \frac{f_y}{E_f\, \varepsilon_{fd}} \tag{7}$$

Eq. (7) represents the ratio of external reinforcement for a balanced fault between concrete and FRP on a given reinforced concrete ductile system. This quantity of reinforcement in particular is defined as ρ_{fb}.

The equation of balanced fault between concrete and external FRP reinforcement is obtained by replacing the value of the equivalent height of compression block from Eq. (3) in (7).

$$\rho_{fb} = \frac{0.85\, \beta_1\, f'_c\, d_f}{E_f\, \varepsilon_{fd}\, d}\left(\frac{\varepsilon_{cu}}{\varepsilon_{cu} + \varepsilon_{fd} + \varepsilon_{bi}}\right) - \rho_s \frac{f_y}{E_f\, \varepsilon_{fd}} \tag{8}$$

By installing an amount of FRP less than the ratio ρ_{fb}, a system governed by the following failure modes is obtained:

- Mode A: Yield of reinforcing steel, followed by rupture of the FRP. ($\varepsilon_{fd}= 0.9 \cdot \varepsilon_{fu}$).
- Mode B: Creep reinforcing steel, followed by debonding or delamination of the FRP system. ($\varepsilon_{fd}< 0.9 \cdot \varepsilon_{fu}$).

3.2.2. Failure Mode C and D: Failure of concrete with steel yield and without steel yield respectively.

Given a reinforced ductile concrete beam which is strengthened beyond the balanced ratio of external reinforcement (ρ_{fb}), such that a failure mode C is obtained (yield of reinforcement followed by crushing of the concrete without external FRP failure). And this continues to strengthen, increasing the amount of external reinforcement reached at the same time: the failure of reinforcing steel and the concrete failure crush without failure FRP system, the amount of external reinforcement at this level is defined as a ratio of external reinforcement balanced by failure mode C ($\rho_{fb,\,C}$).

In this case, both ε_c and ε_s are known, and their values correspond to ε_{cu} and ε_y. Based on this data we can find the different characteristics to determine the value of $\rho_{fb,\,C}$. From the compatibility of deformations in Fig. 1, we have

$$a = \beta_1 \frac{\varepsilon_{cu}.d}{\varepsilon_{cu} + \varepsilon_y} \tag{9}$$

$$\varepsilon_{fe} = \varepsilon_{cu}\left(\frac{d_f - c}{c}\right) - \varepsilon_{bi} \tag{10}$$

By load balancing, we have the following expression:

$$0.85\, f'_c\, b\, a = A_s\, f_y + n_f\, b_f\, t_f\, f_{fe} \tag{11}$$

Substituting Eq. (9) in Eq. (11), and decomposing the value of effective stress in the FRP external reinforcement (f_{fe}), we obtain the following:

$$0.85\, f'_c\ \beta_1 \frac{\varepsilon_{cu}}{\varepsilon_{cu} + \varepsilon_y} = \rho_s\, f_y + \rho_f\ \varepsilon_{fe} E_f \tag{12}$$

Under the hypothesis made ($\rho_f = \rho_{fb,C}$), we obtain the equation of the ratio of external reinforcement balanced by mode C:

$$\rho_{fb,C} = \frac{0.85\, f'_c\ \beta_1}{E_f \varepsilon_{fe}} \left(\frac{\varepsilon_{cu}}{\varepsilon_{cu} + \varepsilon_y} \right) - \frac{\rho_s\, f_y}{E_f \varepsilon_{fe}} \tag{13}$$

The expression of Eq. (13) represents the ratio of external FRP reinforcement at the boundary between failure modes C and D of a beam, given an armed concrete ductile reinforced system. Where, ε_{fe} is obtained from the compatibility relations for the state where concrete and steel fail at the same time.

Given a reinforced concrete beam representing a ductile system, ie the ratio of reinforcing steel is less than its balanced ratio of reinforcement ($\rho_s < \rho_b$) according to considerations of ACI 318 [5]. When the system is reinforced with FRP to meet its deficit resistance of any origin; we can identify the failure mode configuration that is designed (based on the reinforcement system, mechanical characteristics, number of layers, width and thickness of reinforcement used). The diagram in Fig. 02 can be used to identify the failure mode of a concrete reinforced beam externally strengthened with FRP system.

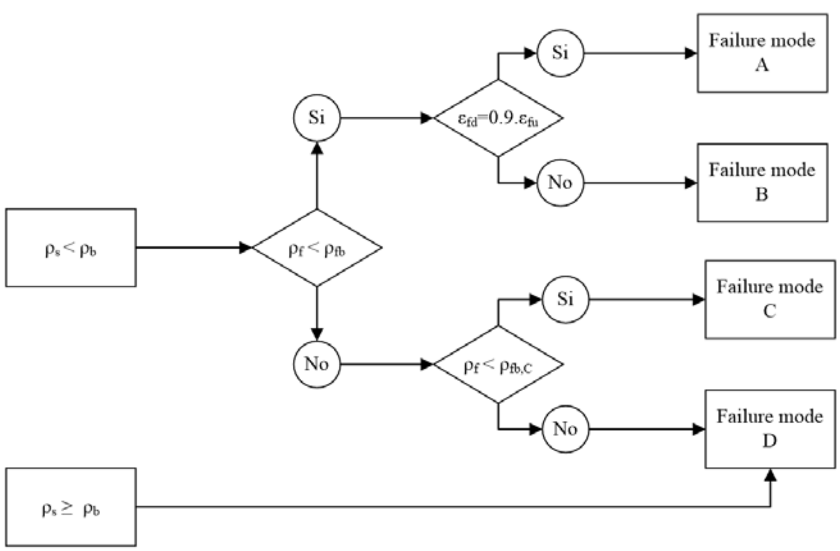

Figure 2: Proposed process for identifying the failure mode of a concrete reinforced beam externally strengthened with an FRP system (Adapted from [4]).

3.3. Ductility analysis of strengthened sections

Sections with failure modes A, B and C are of concern in this analysis since they can develop steel yield before the collapse of the FRP system. An analysis of these reinforced sections will be made in elastic and ultimate states, to determine the ductility of the strengthened system (μ).

$$\mu = \frac{\phi_u}{\phi_y} \tag{14}$$

In a system attached to a failure mode A, B or C, at the instant of steel yield, a graph similar to that shown in Fig. 2 is obtained.

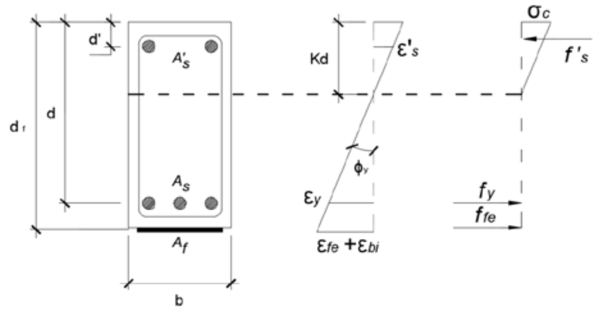

Figure 3: Internal strain and stress distribution for a rectangular beam under bending at elastic limit state.

The curvature of the moment-curvature curve at steel yield can be obtained from Fig. 3 representing the limit of the elastic cracked state of a beam subjected to bending.

$$\phi_y = \frac{f_y/E_s}{d(1-K)} \tag{15}$$

For evaluating Eq. (15), "K" is obtained from the elastic stress-strain relationships for the cracked section (Eq. (16)).

$$K = \sqrt{(n\rho + n\rho' + n_{frp}\,\rho_f)^2 + 2n\left(\rho + \rho'\frac{d'}{d}\right) + 2n_{frp}\,\rho_f\frac{d_f}{d}} - n(\rho' + \rho) - n_{frp}\,\rho_f \tag{16}$$

In failure modes A or B, the last curvature (Fig. 1) during the FRP system failure is obtained with Eq. (17), according to the strain compatibility.

$$\phi_u = \frac{\varepsilon_{fd} + \varepsilon_{bi}}{d_f - {}^{a}/_{\beta_1}} \tag{17}$$

In failure mode C, the last curvature (Fig. 1), during the concrete failure (without FRP system failure), is obtained from Eq. (18), according to the strain compatibility.

$$\phi_u = \frac{\varepsilon_{cu}\beta_1}{a} \tag{18}$$

3.4. Experimental data – Bending test

A series of experimental tests designed for different failure modes have been performed, giving the identification method proposed in Fig. 2. These specimens were built and designed with considerations of ACI 440 guide [6].

3.4.1. Properties of the Specimens

The series of experimental assays took place in the Structures Laboratory of the CISMID (Lima). The experimental test program consisted of a series of tests bending reinforced concrete beams externally reinforced with a CFRP system. The specimens were tested as simply supported beams at their ends.

The beams have a cross section of 200 x 400 mm^2, with a total span of 2700 mm. The beams were reinforced internally with longitudinal bars. The internal steel shear reinforcement consists of closed stirrups to avoid a shear failure. The external FRP's for strengthening are formed by laminated layers of different widths and configurations along the tensile zone by a length of 2.30 m centered along the beam.

There are three trial groups that belong to different researchers, which together make a total of 17 specimens, ranging between non pre-cracked and pre-cracked reinforced concrete beams strengthened with FRP.

Table 1– First group of properties of the tested specimens [4].

Specimen	**Section bxh mm^2**	**Reinforced steel in tension**	**ρ_s %**	**n_f**	**b_f m**	**ρ_f (%)**	**Clear distance m**	**Pre-Cracking**	**$\phi(M_n+\psi M_{nf})$ kN-m**
VF-01	200x400	3 No. 16	0.86	1	0.20	0.29	2.45	No	109
VF-01A	200x400	3 No. 16	0.86	2	0.20	0.58	2.45	Yes	116
VF-01B	200x400	3 No. 16	0.86	3	0.20	0.87	2.45	No	115
VF-02	200x400	4 No.16+1 No.13	1.42	1	0.20	0.31	2.35	No	136
VF-03	200x400	8 No. 16	2.53	3	0.20	0.96	2.45	Yes	135

Table 2– Second group of properties of the tested specimens [7].

Specimen	**Section bxh mm^2**	**Reinforced steel in tension**	**ρ_s %**	**n_f**	**b_f m**	**ρ_f (%)**	**Clear distance m**	**Pre-Cracking**	**$\phi(M_n+\psi M_{nf})$ kN-m**
MB-01	200x400	2 No. 12	0.37	1	0.15	0.04	2.45	No	62
MB-02	200x400	2 No. 12	0.37	1	0.15	0.04	2.45	No	58
MB-03	200x400	2 No. 12	0.37	1	0.15	0.04	2.45	No	55
MB-04	200x400	2 No. 12	0.37	2	0.075	0.04	2.45	No	57
MB-05	200x400	2 No. 12	0.37	2	0.075	0.04	2.45	No	50
SK-01	200x400	2 No. 12	0.37	1	0.10	0.17	2.45	No	61
SK-02	200x400	2 No. 12	0.37	1	0.05	0.09	2.45	No	49
MB-R	200x400	2 No. 12	0.37	1	0.15	0.04	2.45	Yes	59

Table 3– Third group of properties of the tested specimens [8].

Specimen	**Section bxh mm^2**	**Reinforced steel in tension**	**ρ_s %**	**n_f**	**b_f m**	**ρ_f (%)**	**Clear distance m**	**Pre-Cracking**	**$\phi(M_n+\psi M_{nf})$ kN-m**
MB-01'	200x400	2 No. 12	0.37	1	0.15	0.04	2.45	No	62
MB-02'	200x400	2 No. 12	0.37	2	0.075	0.04	2.45	No	53
SK-01'	200x400	2 No. 12	0.37	1	0.15	0.17	2.45	No	67
SK-02'	200x400	2 No. 12	0.37	2	0.05	0.17	2.45	No	63

3.4.2. Material properties

The following materials and specifications were used for the construction of the specimens.

Concrete: The cement used was Portland type I. The specific concrete resistance reached was different for each group. Concrete strength was reviewed by typical standard test concrete cylinders, made 28 to 30 days after casting.

Reinforcing steel: Internal longitudinal strengthening and transverse reinforcement of concrete consisting of corrugated steel bars quality ASTM A615 grade 60.

FRP external strengthening: The external strengthening is placed with longitudinally oriented fibers. The average tensile strength and modulus of elasticity of the laminate according to the method ASTM D-3039 are described in Table 4. The resin used as adhesives corresponds to the same product provider FRP, characterized by its epoxy base and mixed into two components.

Table 4 – Properties of the tested specimens.

Group of tests	f'_c (MPa)	f_y (MPa)	FRP System	E_f (MPa)	t_f (mm)	Epoxy base product
Bazan (2015) [4]	32	420	Tyfo SCH-41	95.8	1.00	Tyfo-S
Rodríguez and Vílchez (2006) [8]	21	420	Mbrace CF130	227	0.17	Mbrace-Saturant
			Sika Carbodur S12	165	1.20	Sikadur-30
Baca and Espinoza (2005) [7]	24	420	Mbrace CF130	227	0.17	Mbrace-Saturant
			Sika Carbodur S12	165	1.20	Sikadur-30

3.4.3. Preparation, test setup and Instrumentation

The bending tests were performed on an assembled steel structure, consisting of a frame which holds the vertical load transmitter and a level base, acting as support for specimens and for the transducers that were placed. Both structures are properly fixed to the rigid foundation of the laboratory.

Furthermore the load transmitter was fixed to a rigid support porch supported by the upper steel beam and braced by a steel beam at the middle portion toward the columns. The instruments used for laboratory testing were composed of the measurement system, the transmitter or load cell and the data acquisition system, according to the stipulations of the technical standard ASTM-C 78 “Standard Test Method for Flexural Strength of Concrete (Using a Simple Beam with Third-Point Loading)”.

4. Experimental Results and Discussion

In terms of the failure mode, the trials considered coincided with the failure predicted by the proposed method, except for the VF-03 test that showed the elastic behavior expected until an unexpected shear failure in one of the supports was produced. In Table 5, the results of experimental failure modes are presented and compared with the modes expected by proposed expressions.

Table 5 - Evaluation of the failure mode for the tests performed.

Beam	n_f	**0.9·ε_{fu} (%)**	**Clamps U**	ε_{fd} **(%)**	**Clamps: (1.3·ε_{fd}) (%)**	ρ_f **(%)**	ρ_{fb} **(%)**	$\rho_{fb,C}$ **(%)**	**Failure Mode expected**	**Experimental failure mode**
VF-01	1	0.9	Yes	0.69	0.90	0.29	0.50	3.28	Mode A	Mode A
VF-01A	2	0.9	Yes	0.54	0.70	0.58	0.87	3.28	Mode B	Mode B
VF-01B	3	0.9	Yes	0.44	0.57	0.87	1.32	3.28	Mode B	Mode B
VF-02	1	0.9	Yes	0.69	0.90	0.30	0.27	2.24	Mode C	Mode C
VF-03	3	0.9	Yes	0.44	0.57	0.97	0.27	0.63	Mode D	Shear
MB-01	1	1.5	Yes	1.03	1.34	0.04	0.12	1.28	Mode B	Mode B
MB-02	1	1.5	No	1.03	1.03	0.04	0.12	1.28	Mode B	Mode B
MB-03	1	1.5	No	0.73	1.03	0.04	0.12	1.28	Mode B	Mode B
MB-04	2	1.5	No	0.73	0.73	0.04	0.26	1.28	Mode B	Mode B
MB-05	2	1.5	No	0.73	0.73	0.04	0.26	1.28	Mode B	Mode B
SK-01	1	1.5	No	0.46	0.46	0.17	0.84	1.76	Mode B	Mode B
SK-02	1	1.5	No	0.46	0.46	0.09	0.84	1.76	Mode B	Mode B
MB-R	1	1.5	Yes	1.03	1.34	0.04	0.12	1.28	Mode B	Mode B
MB-01’	1	1.5	Yes	0.97	1.26	0.04	0.12	1.09	Mode B	Mode B
MB-02’	2	1.5	Yes	0.68	0.89	0.04	0.24	1.09	Mode B	Mode B
SK-01’	1	1.5	Yes	0.43	0.55	0.17	0.80	1.50	Mode B	Mode B
SK-02’	2	1.5	Yes	0.30	0.39	0.17	1.43	1.50	Mode B	Mode B

Table 6 - Summary of results of bending curvature at steel yield and at the ultimate state, and the respective ductility of the beams tested, compared with the theoretical ductility.

Specimen	ρ_s **%**	ρ_f **%**	ρ' **%**	**Experimental** Φ_y **1/m**	**Experimental** Φ_u **1/m**	**μ Experimental**	**μ Theoretical (Eq. (14))**	**Δ Variation of ductility**
VF-01	0.86	0.29	0.15	0.011	0.031	2.82	2.70	-0.12
VF-01A	0.86	0.58	0.15	0.013	0.023	1.74	1.93	0.19
VF-01B	0.86	0.87	0.15	0.008	0.009	1.14	1.58	0.44
VF-02	1.42	0.31	0.15	0.014	0.027	1.94	2.48	0.54
VF-03	2.53	0.96	0.16	-	0.013	-	-	-
MB-01	0.37	0.04	0.21	0.0074	0.0288	3.89	3.71	-0.18
MB-02	0.37	0.04	0.21	0.0093	0.0285	3.06	3.71	0.65
MB-03	0.37	0.04	0.21	0.0054	0.0199	3.68	3.71	0.03
MB-04	0.37	0.04	0.21	0.0090	0.0261	2.90	2.58	-0.32
MB-05	0.37	0.04	0.21	0.0096	0.0210	2.19	2.58	0.39
SK-01	0.37	0.17	0.21	0.0087	0.0102	1.17	1.62	0.45
SK-02	0.37	0.09	0.21	0.0096	0.0126	1.31	1.60	0.29
MB-R	0.37	0.04	0.21	0.0090	0.0390	4.33	3.71	-0.62
MB-01’	0.37	0.04	0.21	0.0063	0.0267	4.24	3.50	-0.74
MB-02’	0.37	0.04	0.21	0.0065	0.0189	2.91	2.43	-0.48
SK-01’	0.37	0.17	0.21	0.0105	0.0146	1.39	1.53	0.14
SK-02’	0.37	0.17	0.21	0.0093	0.0285	3.06	1.05	-
Standard deviation.	s =							0.44

(-) No value.

Based on the information of the tests performed and the respective theoretical approaches developed, we calculated the values of the curvatures in the steel yield and in the ultimate state, and the evaluation of the corresponding ductility. In Table 6, the main results are summarized for different specimens analyzed.

Elimination of most variables results as SK-02', the experimental results are consistent with the tests performed. There is a difference of -0.74 to +0.65 units between experimental and theoretical ductility proposals. We obtained a standard deviation of 0.44 units for variation of ductility (Table 6).

Evaluation of the theoretical expressions and the numerical responses indicates similar results and representations to those obtained with the experimental data, so the theoretical equations (Eqs. (15) to (18)) can be extended to study other FRP system configurations, as one or more layers on both flexible and rigid systems of other products. The use of these expressions will be extended in order to evaluate the expected behavior and properties of failure modes and the amount of reinforcing steel and FRP external reinforcement.

We have developed three graphs with different ratios of reinforcement steel and different ratios and axial stiffness of FRP system, expressing the trend in behavior change, specifically in the ductility and control of steel yield; for concrete quality: 21 MPa, 28 MPa and 35 MPa (Figs. 4 to 6).

In general the inclusion of low ratios of FRP strengthening in reinforced concrete beams derived a more ductile behavior with respect to applying high ratios. This had already been observed by Mukherjee and Joshi [9], who indicated that small ratios of CFRP for strengthening beam-column nodes increase the energy dissipation capacity when compared with high strengthening ratios.

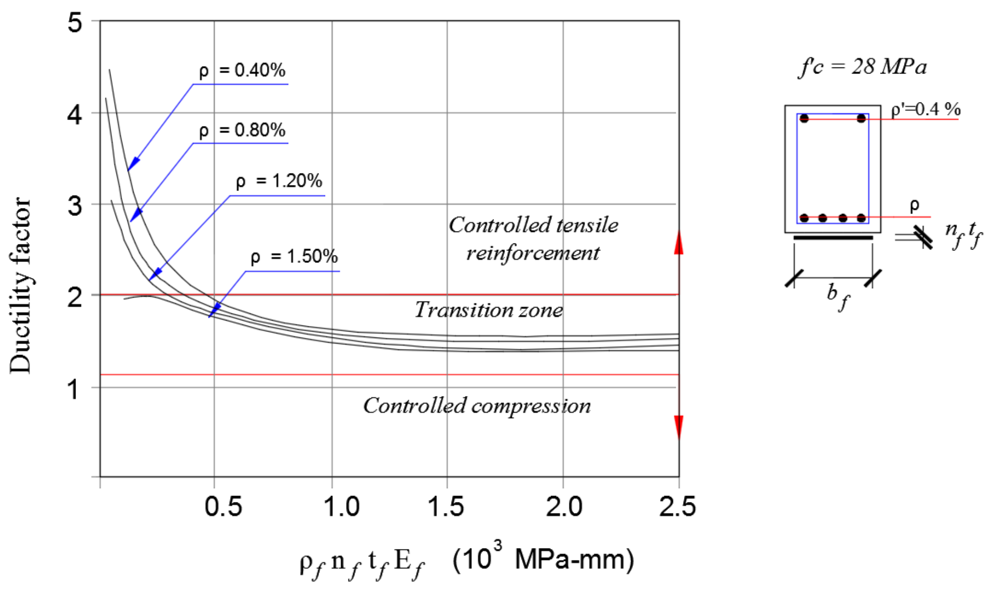

Figure 4: Mean Ductility (μ) versus the product of FRP reinforcing amount and respective axial stiffness ($\rho_f \cdot n_f . t_f . E_f$) for concrete beams with different amounts of reinforcing steel (f'_c = 28 MPa, ε_{bi} = 0.0006).

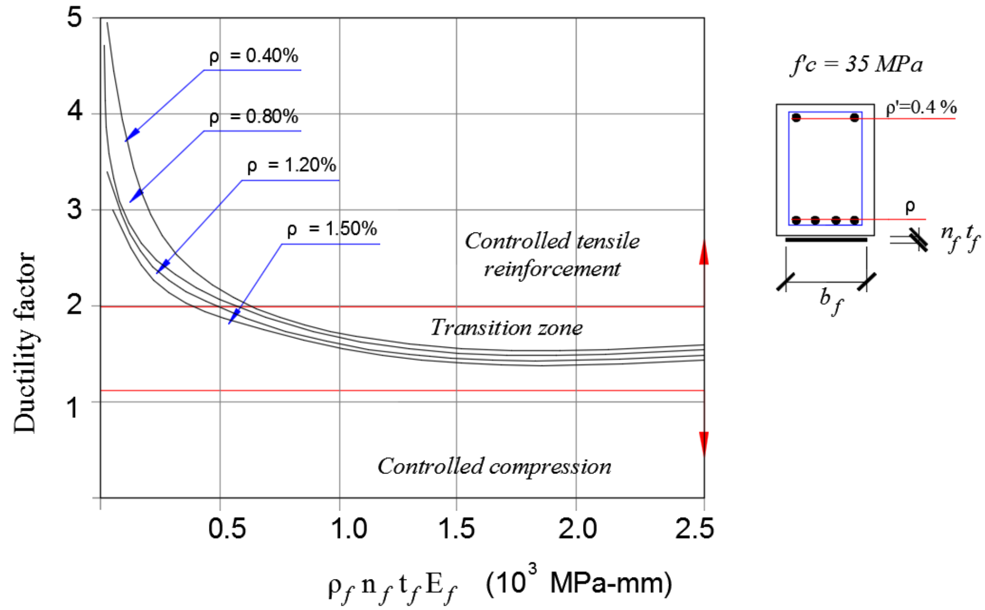

Figure 5: Mean Ductility (μ) versus the product of FRP reinforcing amount and respective axial stiffness ($\rho_f \cdot n_f.t_f.E_f$) for concrete beams with different amounts of reinforcing steel (f'_c = 35 MPa, ε_{bi} = 0.0006).

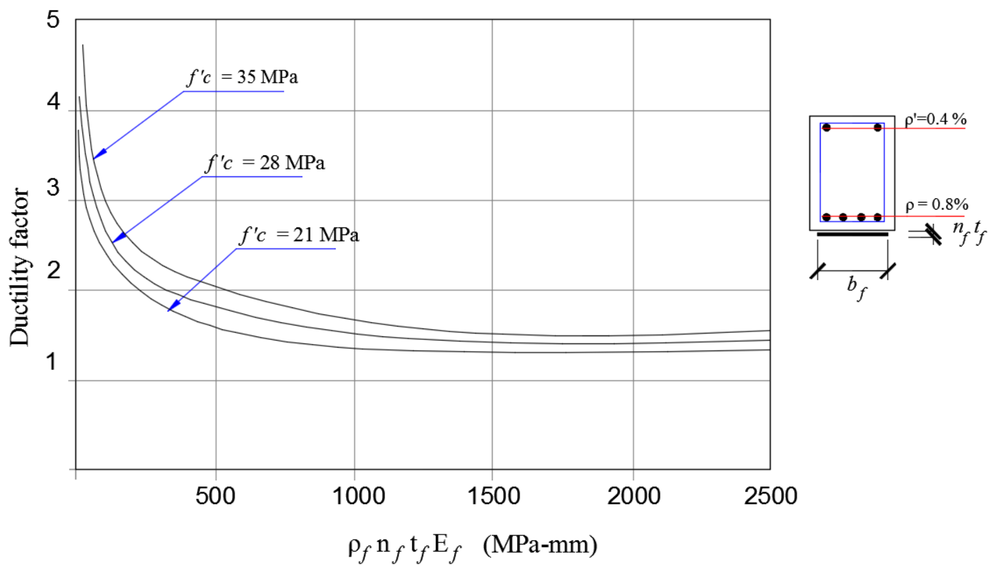

Figure 6: Mean Ductility (μ) versus the product of FRP reinforcing amount and respective axial stiffness ($\rho_f \cdot n_f.t_f.E_f$) for beams with different quality of concrete (ρ_s= 0.8%, ε_{bi}=0.0006).

5. Conclusions

The main conclusions derivate from this study are:

- The final behavior obtained by strengthening a reinforced concrete beam depends primarily on the amount of existing steel reinforcement, the amount of FRP external reinforcement in place, the axial stiffness of the FRP system to be applied, and the quality of the concrete substrate. Other factors that may affect this are the steel reinforcement in compression and the use of U clamps of FRP, etc.

- In ductile reinforced concrete beams, with an applied amount of external strengthening FRP (ρ_f) less than the balanced ratio per fiber (ρ_{fb}) ductile sections can be obtained with a type of fault controlled by FRP, type A or B depending on the final effective strain in the FRP.

- In ductile reinforced concrete beams, with an applied an amount of external strengthening FRP (ρ_f) higher than the balanced ratio per fiber (ρ_{fb}), but also less than the balanced ratio per fiber controlled by type C ($\rho_{fb,C}$), ductile sections can be obtained with a type of fault controlled by steel yield followed by crushing concrete without failure FRP, failure mode C.

- In ductile reinforced concrete beams, with an applied amount of external strengthening FRP (ρ_f) higher than the balanced ratio per fiber controlled by type C ($\rho_{fb,C}$) sections can be obtained with a type of fault controlled by crushing concrete.

- The failure modes of trials of the experimental data presented is consistent with what is expected by the proposed procedure for identifying the failure mode.

- Using designs governed by failure modes A or B can derive a ductility of the order of 1.3 to 4.0 units.

- In sections of beams with a ratio of strengthening ρ_s< 0.80% and concrete quality from 21 to 28 MPa, wherein the product of FRP ratio of strengthening and the axial rigidity of the FRP system ($\rho_f.n_f.t_f.E_f$) to be used is less than 200 MPA-mm, a failure zone controlled by tension and ductility in the range of 2.0 units to more is obtained.

- In sections with existing steel reinforcing ratios ρ_s = 0.40 -1.20% and quality of concrete of 28 MPa, it is possible to obtain, in limited way, a ductile section strengthened externally with FRP.

6. References

[1] Teng J. G., Smith S. T., Yao J. y Chen J. F. (2001): Intermediate Crack Induced Debonding in RC Beams and Slabs. *Construction and Building Materials*, V. 17, No. 6-7

[2] CECS-146. (2003): Technical specification for strengthening concrete structures with carbon fiber reinforced polymer laminate. *China Association for Engineering Construction Standardization*. Beijing

[3] Bank L. (2006): *Composites for Construction: Structural Design with FRP Materials*. John Wiley & Sons, 1ra edition.

[4] Bazán, J. (2015): *Estudio experimental y numérico del comportamiento de flexión de vigas de concreto armado reforzadas con bandas de FRP*. MSc thesis (in Spanish), Universidad Nacional de Ingeniería, Facultad de Ingeniería. Lima, Peru.

[5] ACI Commitee 318. (2014): *Requisitos de Reglamento para Concreto Estructural (ACI 318S-14) y Comentario (318RS-14)*. Farmington Hills.

[6] ACI Comité 440. (2008): "ACI 440-2R-08: Guide for the Design and Construction of Externally Bonded FRP Systems for Strenghening Concrete Structures"

[7] Baca, E. & Espinoza, C. (2005): *Reforzamiento de Estructuras con Fibras de Carbono*. Thesis (in Spanish) to get the title of Civil Engineer. Universidad Ricardo Palma, Facultad de Ingeniería. Lima, Peru.

[8] Vílchez, R. & Rodríguez, A. (2006): *Evaluación de sistemas de reforzamiento en estructuras de concreto para elementos de flexión*. Thesis (In Spanish) to get the title of Civil Engineer. Universidad Ricardo Palma, Facultad de Ingeniería. Lima, Peru.

[9] Mukherjee, A. & Joshi, M. (2005): *FRPC reinforced beam-column joints under cyclic excitation*. ASCE Journal Composite Structures, (**70**), 185-199.